Electron microscopic analysis of different cell types in human pancreatic cancer spheres

TOSHIYUKI ISHIWATA[1], FUMIO HASEGAWA[1], MASAKI MICHISHITA[2], NORIHIKO SASAKI[3],
NAOSHI ISHIKAWA[1], KAIYO TAKUBO[1], YOKO MATSUDA[4], TOMIO ARAI[4] and JUNKO AIDA[1]

[1]Division of Aging and Carcinogenesis, Research Team for Geriatric Pathology,
Tokyo Metropolitan Institute of Gerontology, Tokyo 173-0015; [2]Department of Veterinary Pathology,
School of Veterinary Medicine, Nippon Veterinary and Life Science University, Tokyo 180-8602;
[3]Research Team for Geriatric Medicine (Vascular Medicine), Tokyo Metropolitan Institute of Gerontology;
[4]Department of Pathology, Tokyo Metropolitan Geriatric Hospital and Institute of Gerontology, Tokyo 173-0015, Japan

Abstract. Cancer stem cells (CSCs), which are pluripotent and self-renewable, contribute to the initiation and metastasis of cancer, and are responsible for resistance to chemotherapy and radiation. Pancreatic ductal adenocarcinoma (PDAC) is an aggressive type of cancer that is associated with a high incidence of distant metastasis and recurrence. Sphere formation reveals cell proliferation under nonadherent conditions and is commonly used to identify CSCs; measurements of the number, area and volume of the spheres are used to estimate stemness of PDAC cells. However, detailed morphological analysis of such spheres has not been performed. The aim of the present study was to examine the morphology of spheres isolated from PANC-1 human pancreatic cancer cells via scanning electron microscopy (SEM) and transmission electron microscopy (TEM). PANC-1 cells formed round to irregular oblong spheres within 1 week following seeding in ultra-low-attachment plates. These spheres exhibited higher levels of expression of CSC markers, including nestin, sex determining region Y-box 2, and CD44 containing variant exon 9, compared with adherent cells. SEM analysis revealed that the spheres exhibited a grape-like appearance, harboring cancer cells with smooth or rough surfaces. Similarly, TEM analysis detected cancer cells with varying surface types within the spheres: Those with smooth surfaces, irregular large protrusions, protrusions and a small number of microvilli, and those with many microvilli throughout the entire cell surface. These morphological differences among cancer cells may be indicative of different stages in the differentiation process, from CSCs to non-CSCs, within the spheres.

Introduction

Despite advances in cancer treatments, pancreatic cancer remains one of the most lethal types of malignant tumor. Pancreatic ductal adenocarcinoma (PDAC) is a major histological subtype of pancreatic cancer, comprising 90% of all cases, and is associated with a high mortality rate owing to its aggressive growth and high metastatic rate (1). Surgical treatment offers the only possible cure for PDAC; however, 80% of PDAC patients are inoperable at diagnosis, and the most recently reported overall survival rate for patients with pancreatic cancer is 8% (2). Notably, by the year 2030, pancreatic cancer is expected to become the second-leading cause of cancer-related deaths in the United States, trailing only lung cancer (3).

A cancer stem cell (CSC) is defined as 'a cell within a tumor that possesses the capacity to self-renew and to cause the heterogeneous lineages of cancer cells that comprise the tumor' (4). CSCs constitute a small proportion of cancer cells and possess high tumorigenic potential *in vivo* (5). CSCs, located at the apex of the hierarchy, have the ability to undergo symmetric and asymmetric cell division, enabling them to both self-renew and give rise to the 'differentiated' tumor cell progeny that form the bulk of a tumor. The 'stem cell theory' of cancer implies that CSCs are responsible for tumor initiation, growth, and even metastasis (6). Because CSCs chiefly remain in the G0 phase of the cell cycle, they are less sensitive to radiation and chemotherapy than proliferating cells (5). As such, they are believed to be responsible for tumor recurrence after completion of adjuvant therapy. Researchers therefore regard CSCs as an important potential cancer therapeutic target (7,8).

Three major methods are employed to identify CSCs: Detection of CSC-specific markers, detection of side population (SP) cells, and the sphere formation assay. In the latter assay, the CSCs of PDAC cells form floating colonies when cultivated in ultra-low-attachment dishes (9-11). Notably, after

Correspondence to: Dr Toshiyuki Ishiwata, Division of Aging and Carcinogenesis, Research Team for Geriatric Pathology, Tokyo Metropolitan Institute of Gerontology, 35-2 Sakae-cho, Itabashi-ku, Tokyo 173-0015, Japan
E-mail: tishiwat@tmig.or.jp

transplantation to immunodeficient mice, sphere-forming cells show higher tumor formation rates than adherent cells (12). In a previous study, we reported that nestin, a pancreatic CSC marker, is more highly expressed in the spheres of three PDAC cell lines than in nonsphere cells (13). Moreover, pancreatic cancer cells derived from metastatic foci of immunodeficient mice form a greater number of spheres in low-attachment plates than do their primary tumor counterparts (14). These findings suggest that CSCs are enriched in the spheres and play an important role in the aggressiveness of PDAC. Nevertheless, a thorough study of CSCs and the differentiation of cells from CSCs within spheres has yet to be conducted at the ultramicroscopic level.

In the present study, we therefore analyzed the surface and cross-sections of spheres isolated from a human PDAC cell line, PANC-1, via scanning electron microscopy (SEM) and transmission electron microscopy (TEM). To our knowledge, this is the first report of the ultramicroscopic features of cancer spheres consisting of cells that exhibit varying surface morphologies.

Materials and methods

Human pancreatic cancer cell line. The human pancreatic cancer cell line PANC-1 was obtained from the Cell Resource Center for Biomedical Research Center at the Institute of Development, Aging, and Cancer of Tohoku University (Sendai, Japan). PANC-1 cells were grown in the RPMI 1640 medium supplemented with 10% fetal bovine serum (FBS) at 37°C in a humidified atmosphere containing 5% CO_2.

Sphere-forming assays. For sphere formation, PANC-1 cells (10^3/well) were seeded in 24-well ultra-low-attachment plates (Corning Inc., Kennebunk, ME, USA) in RPMI-1640 supplemented with 10% FBS. After 7 days, the spheres were photographed using a phase contrast microscope (Eclipse TS-100; Nikon Co., Ltd., Tokyo, Japan). The spheres were then aspirated using micropipettes and placed into microcentrifuge tubes.

Reverse transcription-quantitative polymerase chain reaction (RT-qPCR). Total RNA was isolated from cells, using an RNeasy Plus Mini kit (Qiagen, Venlo, The Netherlands), and subsequently reverse-transcribed to cDNA, using a ReverTra Ace® qPCR RT kit (Toyobo, Osaka, Japan) according to the manufacturer's protocol. qPCR was performed using a Power SYBR® Green kit (Applied Biosystems; Thermo Fisher Scientific, Inc., Waltham, MA, USA) and a StepOnePlus™ real-time PCR system (Applied Biosystems; Thermo Fisher Scientific, Inc.). Expression of β-actin was considered an internal control. The primer sets used for qPCR analyses are listed in Table I. Gene expression measurements were performed in triplicate.

TEM. Spheres from PANC-1 cells were fixed with 2.5% glutaraldehyde in 0.1 M phosphate buffer (pH 7.4), then postfixed for 1 h with 2% OsO_4 dissolved in distilled water, dehydrated in a graded series of ethanol solutions, and embedded in Epon. Ultrathin sections were generated using an ultramicrotome and stained with uranyl acetate and lead citrate for examination

under a transmission electron microscope (H-7500; Hitachi High-Technologies, Tokyo, Japan).

SEM. Spheres from PANC-1 cells were fixed for 1 h with 2.5% glutaraldehyde in 0.1 M phosphate buffer (pH 7.4) at room temperature and then incubated at 4°C overnight. The following day, the glutaraldehyde solution was removed and the spheres were washed with PBS. After complete dehydration via a graded ethanol series, sphere samples suspended in 100% ethanol were placed onto a Nanopercolator (JEOL Ltd., Tokyo, Japan) and air-dried, then coated with a platinum layer using an MSP-1S sputter coater (Shinku Device, Ibaraki, Japan) and examined and photographed using a Phenom Pro X desktop scanning electron microscope (Phenom-World BV, Eindhoven, The Netherlands) (15,16).

Statistical analysis. Quantitative data are presented as means ± standard deviations. Differences between two groups were analyzed by Student's t-test. P<0.05 was considered to indicate a statistically significant difference. Computations were performed using Microsoft Excel 2010 (Microsoft Corporation, Redmond, WA, USA).

Results

Spheres of PANC-1 cells in ultra-low-attachment plates. After 7 days of incubation in ultra-low-attachment dishes, we observed sphere formation in all 24-wells of each plate, with each well containing approximately 10 spheres (Fig. 1A). Moreover, the PANC-1 cells proliferated and formed irregular, oblong spheres. While certain individual cells could be seen clearly (Fig. 1B, middle to lower parts), others appeared grouped together, making their margins difficult to distinguish under the phase contrast microscope (Fig. 1B, upper part).

RT-qPCR. To confirm the stemness of the PANC-1 spheres, we screened the spheres for expression of CSC markers, including Oct4, sex determining region Y-box 2 (Sox2), nestin, CD24, and CD44v9 (7,17-19). Notably, the mRNA expression level of each of these markers was higher in PANC-1 spheres than in adherent cells (Fig. 2A-E). In particular, *Sox2* was expressed at 4-fold higher levels in spheres than in adherent cells, which was the largest fold-difference observed.

SEM analysis of spheres from PANC-1 cells. Low-magnification SEM imaging showed that the spheres of PANC-1 cells exhibited an oval to club-like appearance. The surface of the sphere was rugged, and some cells were fused. The center was smooth, while the periphery contained both smooth and protruding areas (Fig. 3A). Additionally, at high-magnification, the spheres had a grape-like appearance, with a mostly smooth surface and rough-surfaced PANC-1 cells (Fig. 3B). We observed a small hole in the surface of certain PANC-1 cells (arrow), and some sphere cells showed several irregular protrusions on their surfaces (Fig. 3C), while others appeared to be fused, with unclear margins.

TEM analysis of spheres from PANC-1 cells. Low-magnification TEM indicated that PANC-1 cells

Table I. List of primer sets for reverse transcription-quantitative polymerase chain reaction.

Gene	Forward primer (5'-3')	Reverse primer (5'-3')
Nestin	TCCTGCTGTAGATGCAGAGATCAG	ACCCTGTGTCTGGAGCAGAGA
Sox2	TGCGAGCGCTGCACAT	TCATGAGCGTCTTGGTTTTCC
CD44v9	AGCAGAGTAATTCTCAGAGCTT	TGCTTGATGTCAGAGTAGAAGT
β-actin	GGTCATCACCATTGGCAATGAG	TACAGGTCTTTGCGGATGTCC

Sox2, sex determining region Y-box 2; CD44v9, CD44 containing variant exon 9.
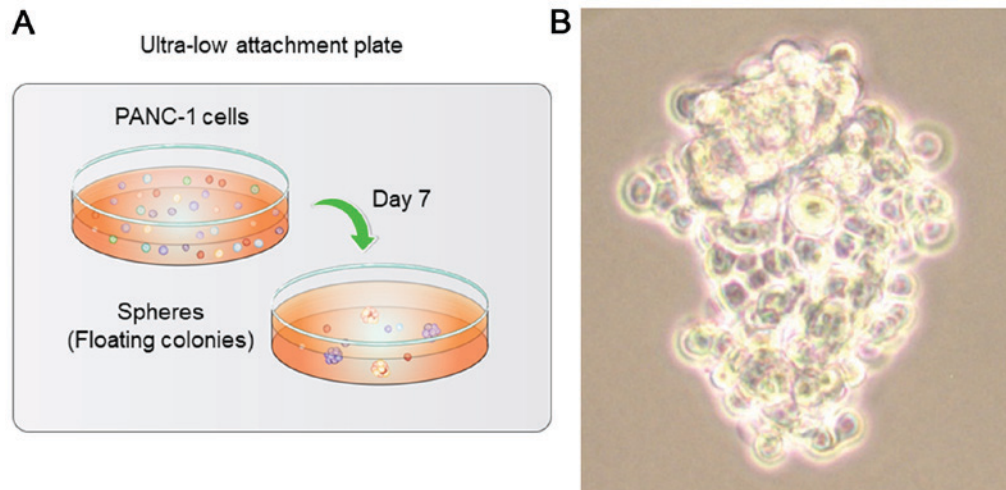
Figure 1. Spheres of the PANC-1 human pancreatic cancer cell line, in ultra-low-attachment plates. (A) Schematic of sphere formation by PANC-1 cells in the ultra-low-attachment plates. (B) A phase contrast image of a PANC-1 cell sphere. Magnification, x200.
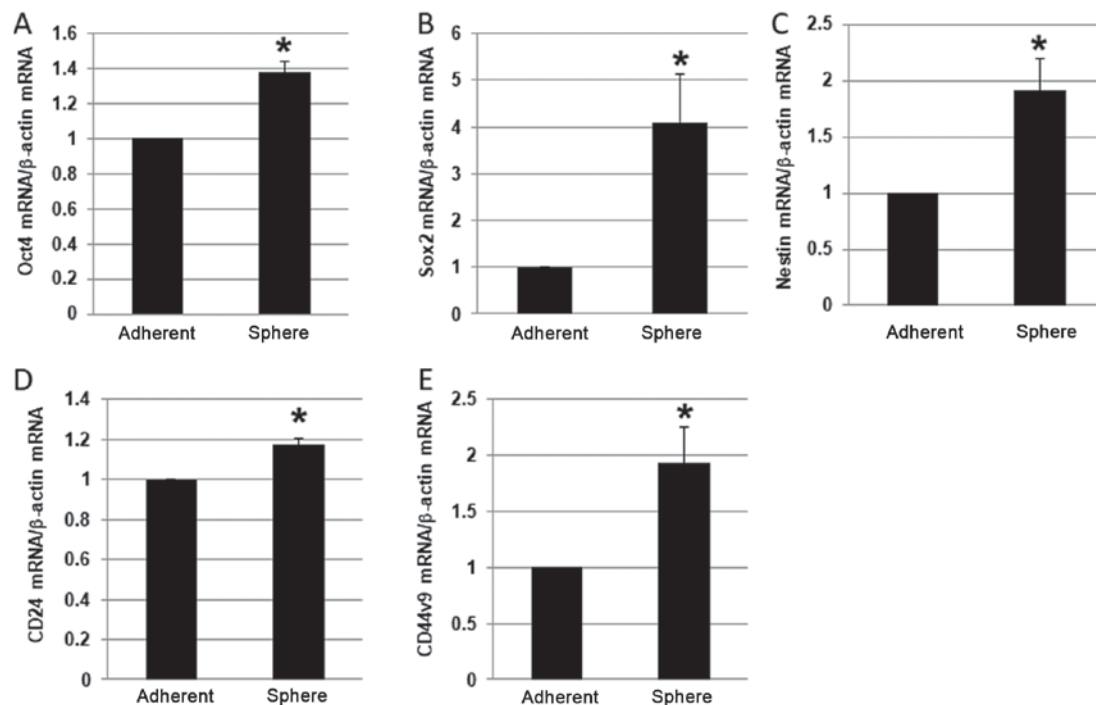

Figure 2. Expression of cancer stem cell markers in adherent PANC-1 cells and spheres. Reverse transcription-quantitative polymerase chain reaction analysis was performed using cDNA derived from adherent and sphere cells to determine the expression of the stem cell markers, (A) Oct4, (B) Sox2, (C) Nestin, (D) CD24 and (E) CD44v9. The results were obtained following normalization against the values obtained for adherent cells (value=1). Results are presented as the mean ± standard deviations of three independent experiments. *$P<0.05$ vs. adherent cells. Oct4, octamer-binding transcription factor 4; Sox2, sex determining region Y-box 2; CD44v9, CD44 containing variant exon 9.
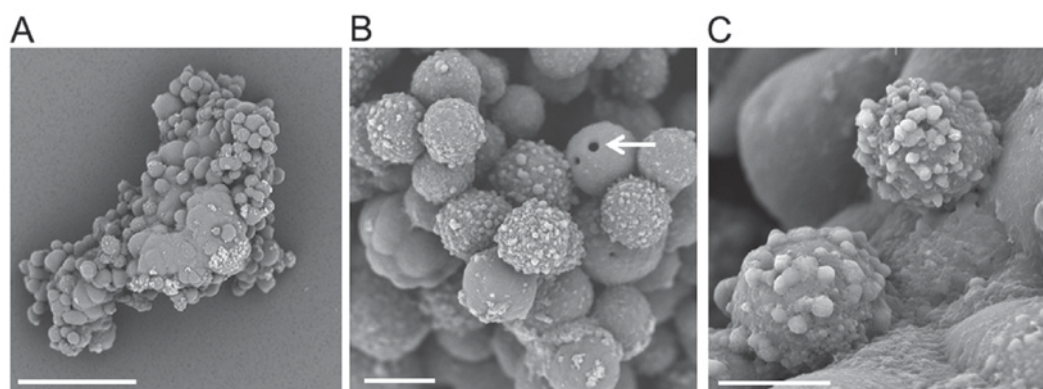
Figure 3. SEM analysis of PANC-1 cell sphere. (A) Low-magnification SEM images of a PANC-1 cell sphere. The sphere has an oblong/club-like appearance; the center is smooth, while the periphery contains smooth and protruding areas. Scale bar=80 μm. (B) High-magnification SEM images of PANC-1 spheres. The cell spheres have a grape-like appearance, and cancer cells have a smooth or rough surface. The arrow indicates a small hole through the surface of the PANC-1 cells. Scale bar=20 μm. (C) Cells located on the outside of the sphere exhibit irregular protrusions at their surface. Scale bar=8 μm. SEM, scanning electron microscopy.
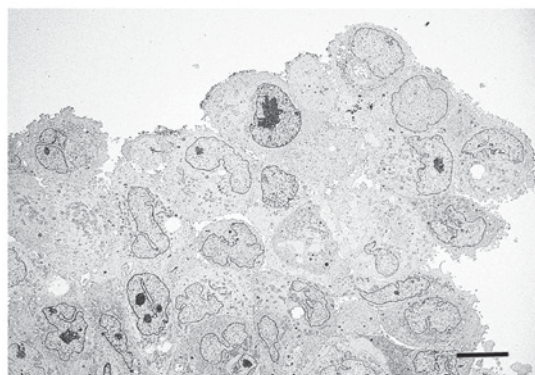

Figure 4. Low-magnification transmission electron microscopy analysis of PANC-1 spheres. Images showing PANC-1 cells that formed spheres with irregular-shaped nuclei and nucleoli, as well as PANC-1 cells with varying cell surfaces. Scale bar=10 μm.
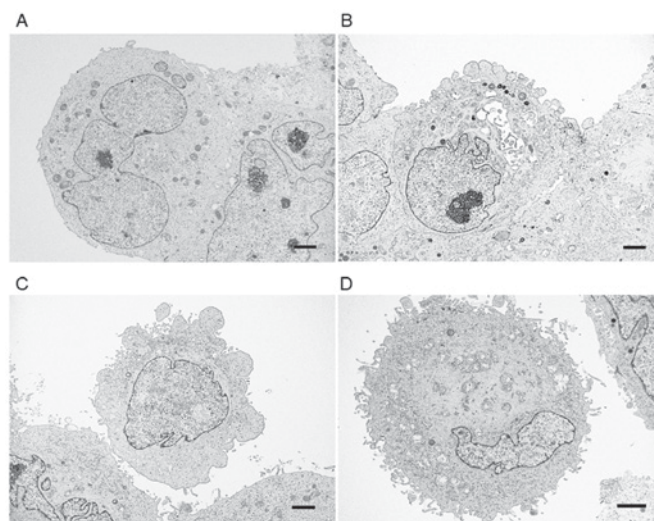

Figure 5. High-magnification transmission electron microscopy analysis of PANC-1 spheres. Images depicting the distinct surface types of cancer cells within spheres, including (A) smooth surface, (B) surface with round protrusions, (C) surface containing protrusions with microvilli, and (D) microvilli located throughout the entire cell surface. Scale bars=2 μm.

formed spheres with irregular-shaped nuclei and nucleoli, and that the cell-to-cell border was not clear in some cells (Fig. 4). Additionally, there were small clefts or cavities between PANC-1 cells in each sphere, and several cells displayed irregular protrusions on their surface. The surface of the PANC-1 cells in spheres was classified into four types: Smooth surface (Fig. 5A), irregular large protrusions (Fig. 5B), protrusions and a small number of microvilli (Fig. 5C), and many microvilli located throughout the entire cell surface (Fig. 5D). Most of the cells with smooth surfaces were located inside the spheres and tightly attached to other cells. Conversely, those with protrusions and microvilli, as well as those exhibiting large numbers of microvilli throughout the surface (Fig. 5C and D), were located at the outside of the spheres, with loose adhesion to other cancer cells.

Discussion

Spheres of PDAC cells represent round aggregates of fused cells formed during the early stage of culture in ultra-low-attachment plates, according to phase contrast microscopic examination. Subsequently, these spheres grow and form irregular, oblong to club-shaped floating colonies. There are several reports of the electron microscopic analysis of cancer spheres or spheroids, involving the hanging-drop method, culture on a scaffold, or culture in low-attachment plates (20,21). SEM images of PANC-1 cells in hanging-drop experiments show a ruffled surface and lightly packed cells with deep pore-like structures (22). The heterogeneous morphology of PDAC spheres consisting of cancer cells is similar to that of morphologically and functionally heterogeneous neurospheres (consisting of neural stem cells and their progeny), which can differentiate into glial cells, neurons, and oligodendrocytes (23,24). The most immature clonogenic cells are located in the core of the neurosphere, whereas progeny and differentiated cells are located at the periphery (25,26). In the present study, we found that the fused cell aggregates are located in the core region of the PDAC spheres, while clearly separated cancer cells exist around the spheres.

In this study, we used serum-containing medium because PANC-1 cells most rapidly form large spheres under these conditions. The spheres generated from these cells expressed high mRNA levels of CSC markers, suggesting that they contain CSCs (7,13,17-19). A previous study showed that PANC-1 cells grown in a serum-containing medium formed clusters that were heterogeneous for dye efflux, while cells grown in the serum-free medium with supplements commonly used to culture stem cells gave rise to colonies that varied in their ability to efflux dye and respond to verapamil (27). In neurospheres, mitotic cells were found at the periphery but not in the inner part of the spheres (23). Growth factors or serum added to the medium might therefore play important roles in the differentiation of the cancer cells on the outside of the spheres, as well as the growth of cells in the spheres.

Our EM analyses detected four types of cancer cells within PDAC spheres. Those with a smooth surface were located inside the spheres and were fused to each other. In contrast, the cells containing protrusions and/or microvilli on their surface were localized at the periphery of the spheres. In a healthy human pancreas, short microvilli are present on acinar cells and ductal epithelial cells (28). Furthermore, PDAC cells are comprised of epithelial cells that form lumens, apical mucin granules, intermediate filaments, tight junctions, and microvilli. In commonly used 2D culture, PANC-1 cells have microvilli on their cell surface (29). SEM and TEM analyses in the present study suggest that the cells with a smooth surface are CSCs of PANC-1, while those with large protrusions, with protrusions and some microvilli, and with large numbers of microvilli on their surfaces represent distinct stages of the differentiation process of pancreatic CSCs to non-CSCs. A recent study showed that lung adenocarcinoma cells can divide into two cell types: Tumor cells and support cells that form a part of a supporting microenvironment known as the niche (30). Further studies are needed to clarify the function of the different types of pancreatic cancer cells in the spheres that were observed in our study.

Here, we identified different types of cells present in spheres formed by a human pancreatic cancer cell line, via EM analysis. The cancer cells exhibited smooth surfaces, rounded protrusions on the cell surface, surfaces containing protrusions with a small number of microvilli, or the presence of large numbers of microvilli across the entire cell surface. These findings suggest that CSCs and differentiated non-CSCs have characteristic morphologies. However, further studies are needed to clarify correlations between cell surface features and cell types within pancreatic cancer spheres.

Acknowledgements

References

1. Jemal A, Siegel R, Ward E, Hao Y, Xu J, Murray T and Thun MJ: Cancer statistics, 2008. CA Cancer J Clin 58: 71-96, 2008.
2. Siegel RL, Miller KD and Jemal A: Cancer statistics, 2016. CA Cancer J Clin 66: 7-30, 2016.
3. Rahib L, Smith BD, Aizenberg R, Rosenzweig AB, Fleshman JM and Matrisian LM: Projecting cancer incidence and deaths to 2030: The unexpected burden of thyroid, liver and pancreas cancers in the United States. Cancer Res 74: 2913-2921, 2014.
4. Clarke MF, Dick JE, Dirks PB, Eaves CJ, Jamieson CH, Jones DL, Visvader J, Weissman IL and Wahl GM: Cancer stem cells-perspectives on current status and future directions: AACR workshop on cancer stem cells. Cancer Res 66: 9339-9344, 2006.
5. Lonardo E, Hermann PC and Heeschen C: Pancreatic cancer stem cells-update and future perspectives. Mol Oncol 4: 431-442, 2010.
6. Reya T, Morrison SJ, Clarke MF and Weissman IL: Stem cells, cancer and cancer stem cells. Nature 414: 105-111, 2001.
7. Matsuda Y, Kure S and Ishiwata T: Nestin and other putative cancer stem cell markers in pancreatic cancer. Med Mol Morphol 45: 59-65, 2012.
8. Ishiwata T: Cancer stem cells and epithelial-mesenchymal transition: Novel therapeutic targets for cancer. Pathol Int 66: 601-608, 2016.
9. Gou S, Liu T, Wang C, Yin T, Li K, Yang M and Zhou J: Establishment of clonal colony-forming assay for propagation of pancreatic cancer cells with stem cell properties. Pancreas 34: 429-435, 2007.
10. Gaviraghi M, Tunici P, Valensin S, Rossi M, Giordano C, Magnoni L, Dandrea M, Montagna L, Ritelli R, Scarpa A and Bakker A: Pancreatic cancer spheres are more than just aggregates of stem marker-positive cells. Biosci Rep 31: 45-55, 2011.
11. Yin T, Wei H, Gou S, Shi P, Yang Z, Zhao G and Wang C: Cancer stem-like cells enriched in Panc-1 spheres possess increased migration ability and resistance to gemcitabine. Int J Mol Sci 12: 1595-1604, 2011.
12. Michishita M, Akiyoshi R, Yoshimura H, Katsumoto T, Ichikawa H, Ohkusu-Tsukada K, Nakagawa T, Sasaki N and Takahashi K: Characterization of spheres derived from canine mammary gland adenocarcinoma cell lines. Res Vet Sci 91: 254-260, 2011.
13. Matsuda Y, Ishiwata T, Yoshimura H, Yamashita S, Ushijima T and Arai T: Systemic administration of small interfering RNA targeting human nestin inhibits pancreatic cancer cell proliferation and metastasis. Pancreas 45: 93-100, 2016.
14. Matsuda Y, Yoshimura H, Ueda J, Naito Z, Korc M and Ishiwata T: Nestin delineates pancreatic cancer stem cells in metastatic foci of NOD/Shi-scid IL2Rγ (null) (NOG) mice. Am J Pathol 184: 674-685, 2014.
15. Konings J, Hoving LR, Ariens RS, Hethershaw EL, Ninivaggi M, Hardy LJ, de Laat B, Ten Cate H, Philippou H and Govers-Riemslag JW: The role of activated coagulation factor XII in overall clot stability and fibrinolysis. Thromb Res 136: 474-480, 2015.
16. Schurgers E, Moorlag M, Hemker C, Lindhout T, Kelchtermans H and de Laat B: Thrombin generation in zebrafish blood. PLoS One 11: e0149135, 2016.
17. Sharma N, Nanta R, Sharma J, Gunewardena S, Singh KP, Shankar S and Srivastava RK: PI3K/AKT/mTOR and sonic hedgehog pathways cooperate together to inhibit human pancreatic cancer stem cell characteristics and tumor growth. Oncotarget 6: 32039-32060, 2015.
18. Herreros-Villanueva M, Zhang JS, Koenig A, Abel EV, Smyrk TC, Bamlet WR, de Narvajas AA, Gomez TS, Simeone DM, Bujanda L and Billadeau DD: SOX2 promotes dedifferentiation and imparts stem cell-like features to pancreatic cancer cells. Oncogenesis 2: e61, 2013.
19. Kiuchi S, Ikeshita S, Miyatake Y and Kasahara M: Pancreatic cancer cells express CD44 variant 9 and multidrug resistance protein 1 during mitosis. Exp Mol Pathol 98: 41-46, 2015.
20. Breslin S and O'Driscoll L: The relevance of using 3D cell cultures, in addition to 2D monolayer cultures, when evaluating breast cancer drug sensitivity and resistance. Oncotarget 7: 45745-45756, 2016.

21. Ishiwata T, Teduka K, Yamamoto T, Kawahara K, Matsuda Y and Naito Z: Neuroepithelial stem cell marker nestin regulates the migration, invasion and growth of human gliomas. Oncol Rep 26: 91-99, 2011.
22. Ware MJ, Colbert K, Keshishian V, Ho J, Corr SJ, Curley SA and Godin B: Generation of homogenous three-dimensional pancreatic cancer cell spheroids using an improved hanging drop technique. Tissue Eng Part C Methods 22: 312-321, 2016.
23. Bez A, Corsini E, Curti D, Biggiogera M, Colombo A, Nicosia RF, Pagano SF and Parati EA: Neurosphere and neurosphere-forming cells: Morphological and ultrastructural characterization. Brain Res 993: 18-29, 2003.
24. Gage FH: Mammalian neural stem cells. Science 287: 1433-1438, 2000.
25. Ilieva M and Dufva M: SOX2 and OCT4 mRNA-expressing cells, detected by molecular beacons, localize to the center of neurospheres during differentiation. PLoS One 8: e73669, 2013.
26. Suslov ON, Kukekov VG, Ignatova TN and Steindler DA: Neural stem cell heterogeneity demonstrated by molecular phenotyping of clonal neurospheres. Proc Natl Acad Sci USA 99: 14506-14511, 2002.
27. Bhagwandin VJ and Shay JW: Pancreatic cancer stem cells: Fact or fiction? Biochim Biophys Acta 1792: 248-259, 2009.
28. Hruban RH, Pitman MB and Klimstra DS: Ductal adenocarcinoma. In: Tumors of the Pancreas. Atlas of Tumor Pathology, 4th series. Silverberg SG and Sobin LH (eds). American Registry of Pathology, Washington, DC, pp111-164, 2007.
29. Lu Y, Onda M, Uchida E, Yamamura S, Yanagi K, Matsushita A, Kobayashi T, Fukuhara M, Aida K and Tajiri T: The cytotoxic effects of bile acids in crude bile on human pancreatic cancer cell lines. Surg Today 30: 903-909, 2000.
30. Tammela T, Sanchez-Rivera FJ, Cetinbas NM, Wu K, Joshi NS, Helenius K, Park Y, Azimi R, Kerper NR, Wesselhoeft RA, *et al*: A Wnt-producing niche drives proliferative potential and progression in lung adenocarcinoma. Nature 545: 355-359, 2017.